Supporting Information for

Hydrology and Earth System Sciences

for the manuscript

Hierarchical sedimentary architecture governs basin-scale solute dispersion: From pre-asymptotic dynamics to uncertainty propagation

Wanli Ren¹, Yue Fan², Anwen Pan¹, Heng Dai^{1*}, Jing Yang³, Mohamad Reza Soltanian⁴, Zhenxue Dai^{5, 6}, Songhu Yuan¹

- ¹ State Key Laboratory of Geomicrobiology and Environmental Changes, China University of Geosciences, Wuhan, Hubei, 430074, China.
- ² Key Laboratory of Geotechnical Mechanics and Engineering of Ministry of Water Resources, Changjiang River Scientific Research Institute, Wuhan, Hubei, 430010, China.
- ³ School of Land Engineering, Chang'an University, Xi'an, Shanxi, 710064, China.
- ⁴ Departments of Geosciences and Environmental Engineering, University of Cincinnati, Cincinnati, Ohio, 45221, USA.
- ⁵ College of Environmental and Municipal Engineering, Qingdao University of Technology, Qingdao, Shandong, 266033, China.
- ⁶ College of Construction Engineering, Jilin University, Changchun, Jilin, 130061, China.

Corresponding author*: Heng Dai (daiheng@cug.edu.cn);

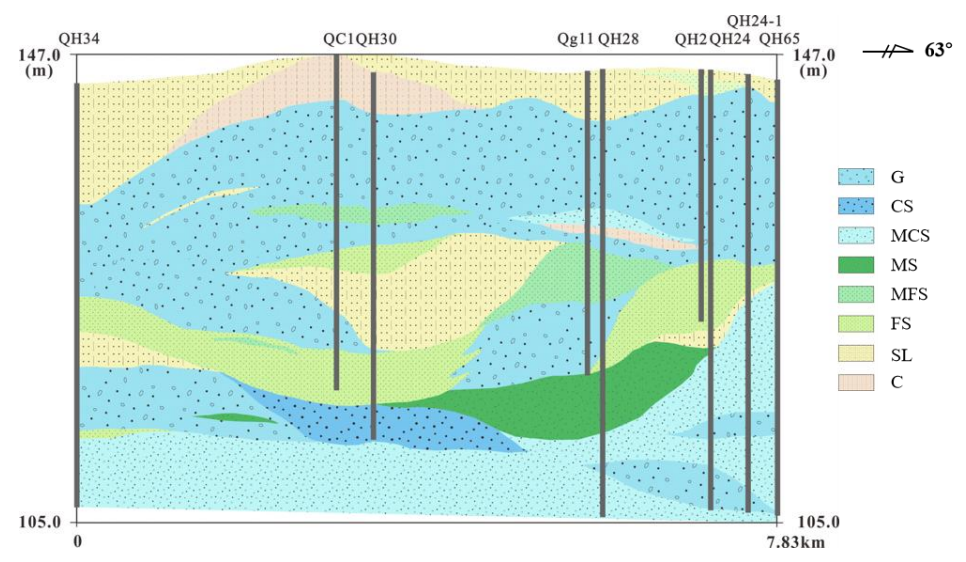


Figure S1. Small-scale lithofacies distribution map on cross-section 1.

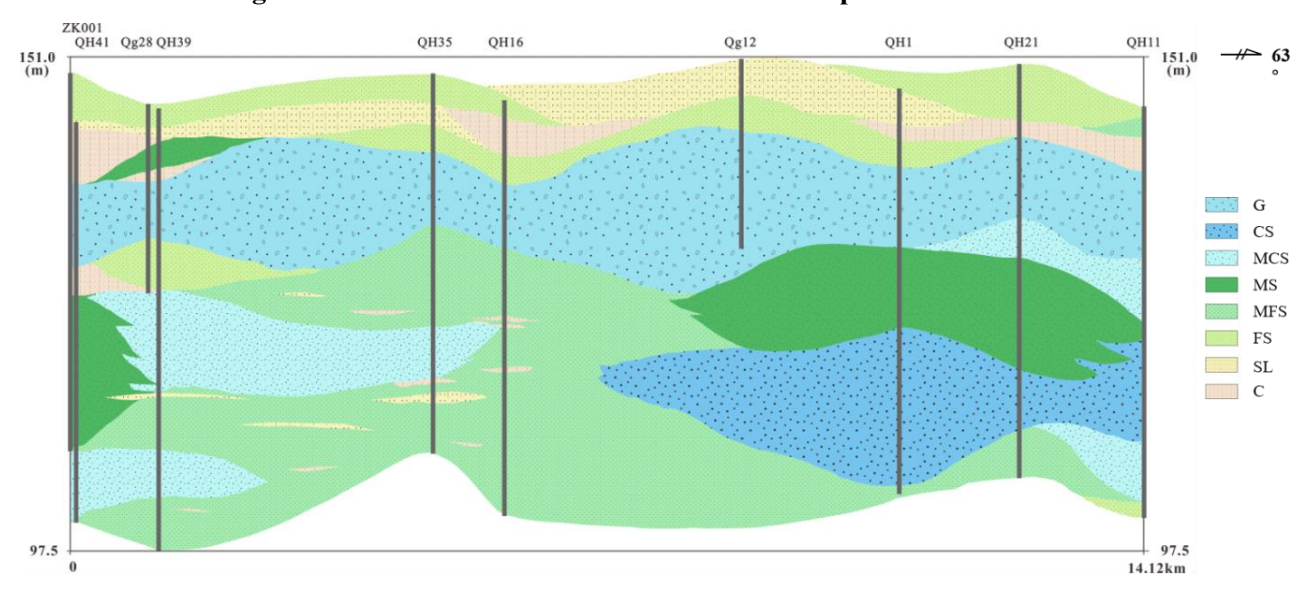


Figure S2. Small-scale lithofacies distribution map on cross-section 2.

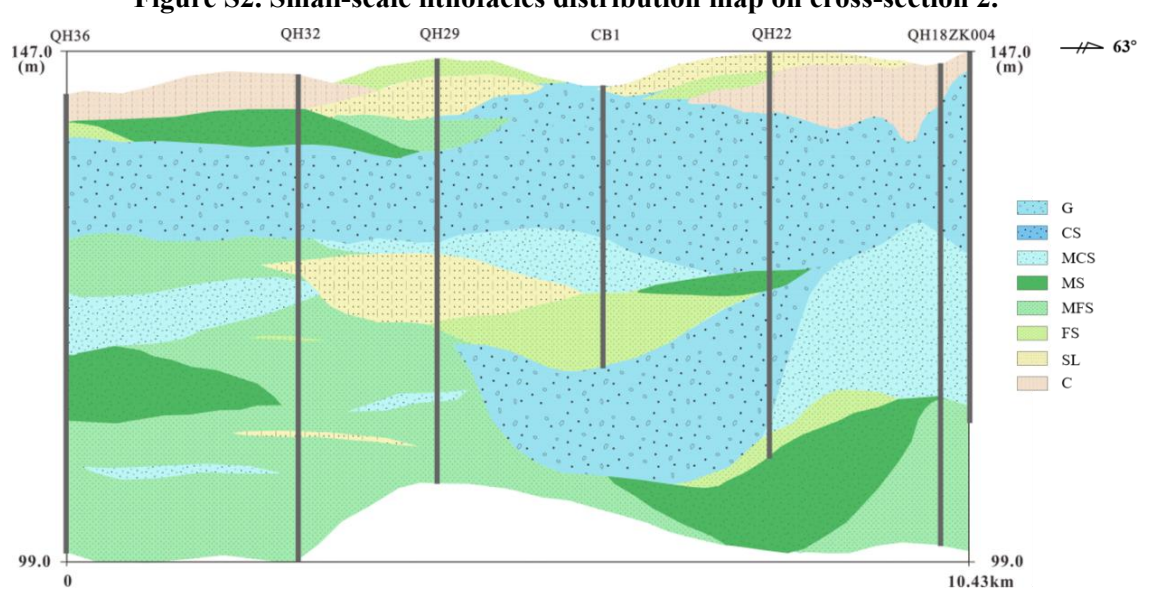


Figure S3. Small-scale lithofacies distribution map on cross-section 3.

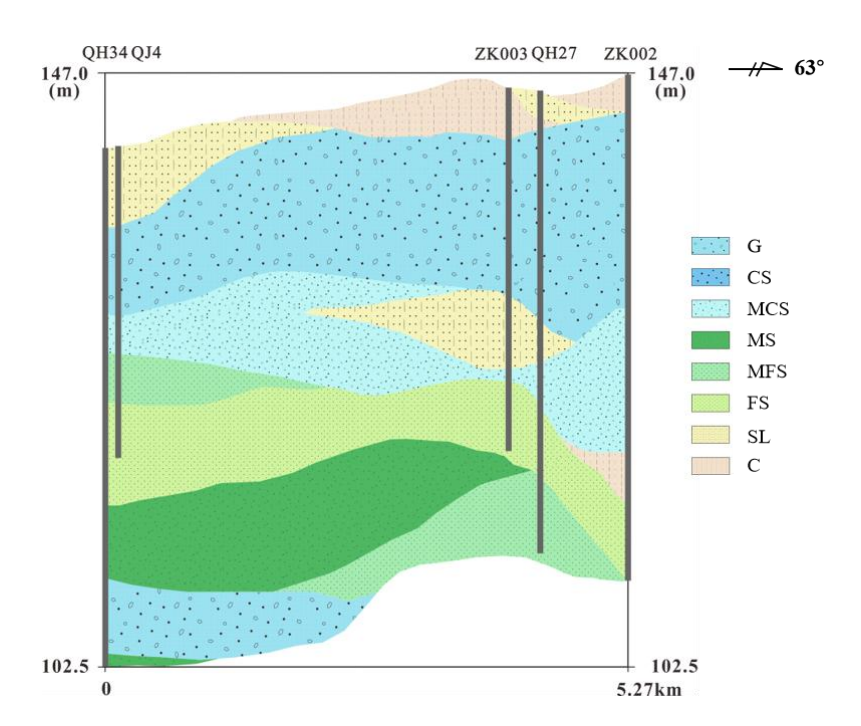


Figure S4. Small-scale lithofacies distribution map on cross-section 4.

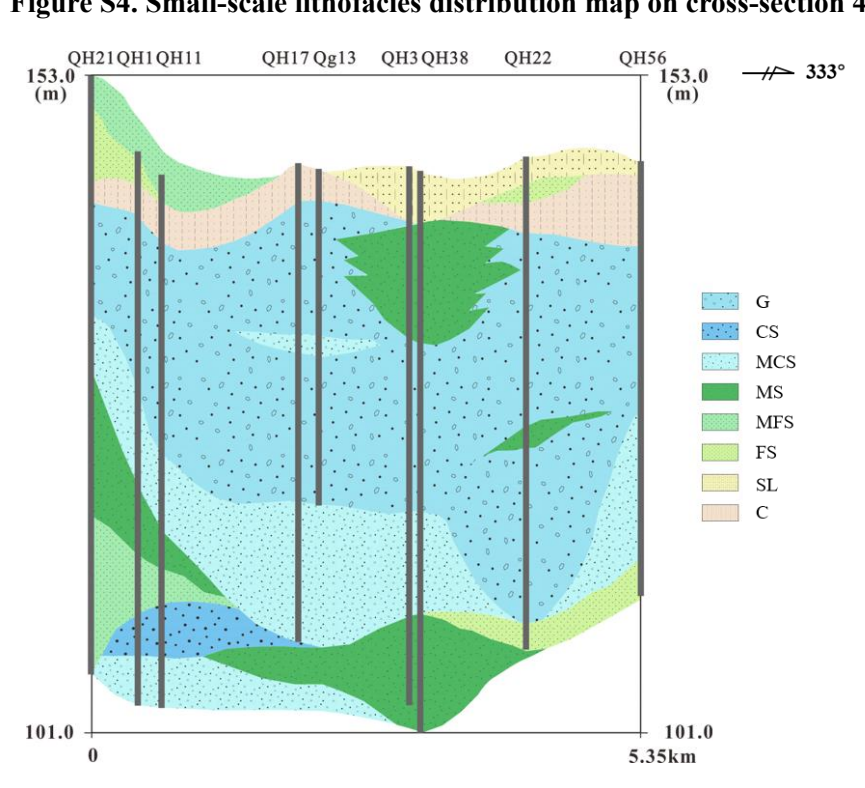
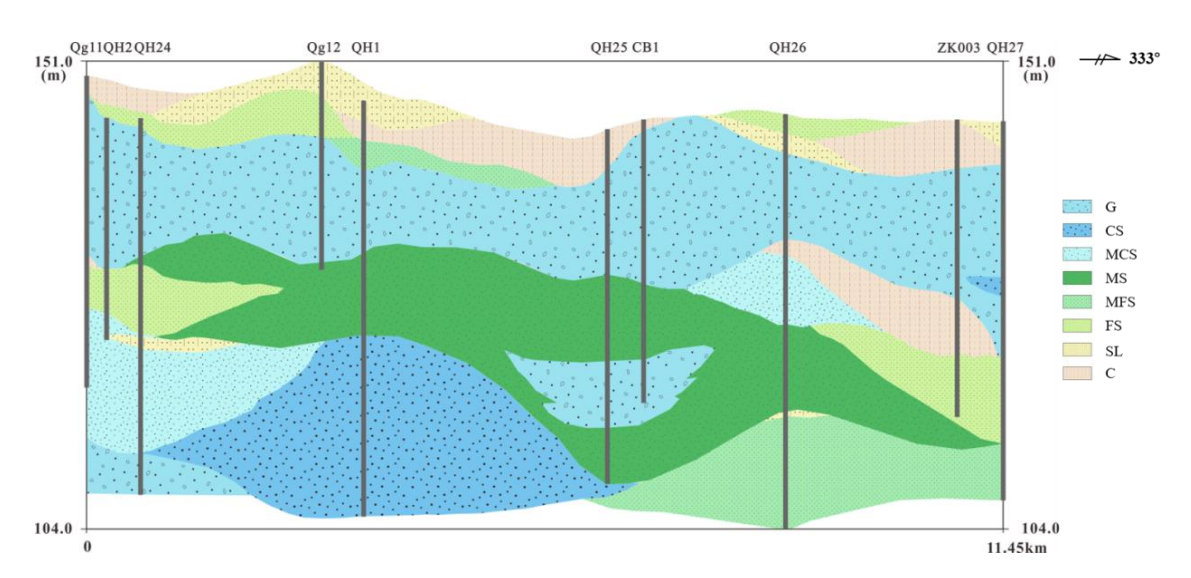


Figure S5. Small-scale lithofacies distribution map on cross-section 5.



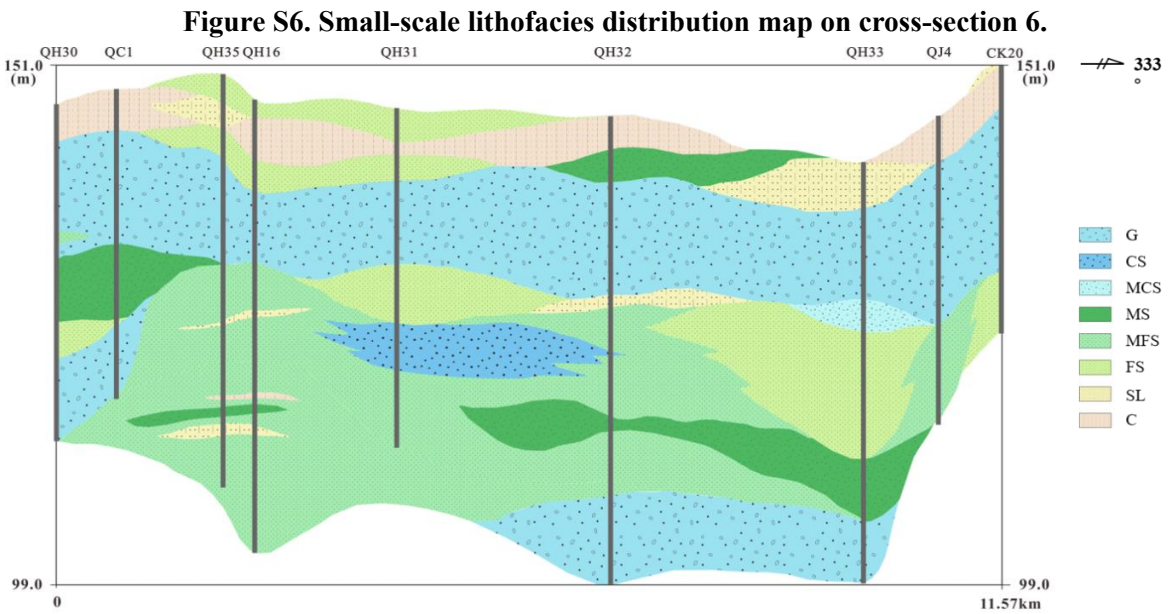


Figure S7. Small-scale lithofacies distribution map on cross-section 7.

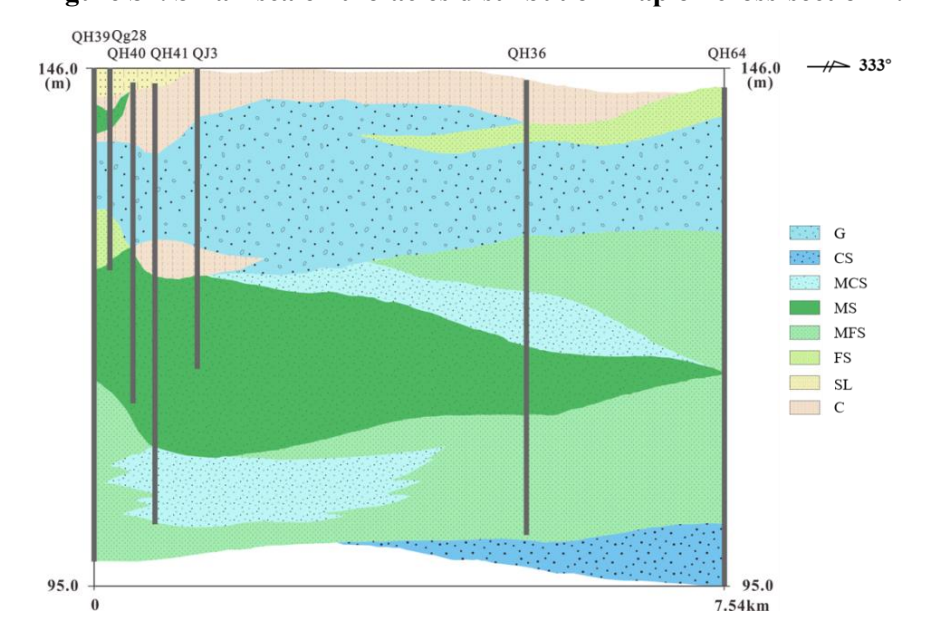


Figure S8. Small-scale lithofacies distribution map on cross-section 8.

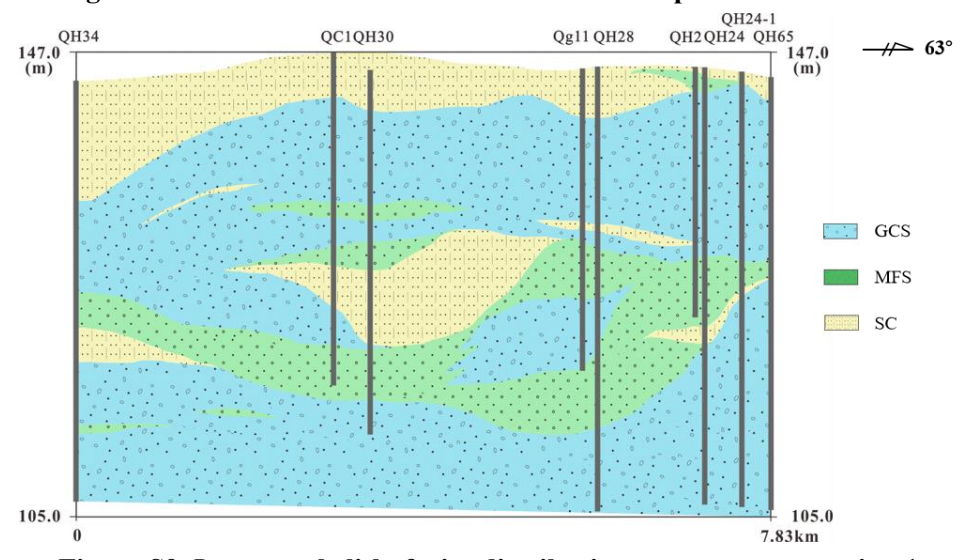


Figure S9. Large-scale lithofacies distribution map on cross-section 1.

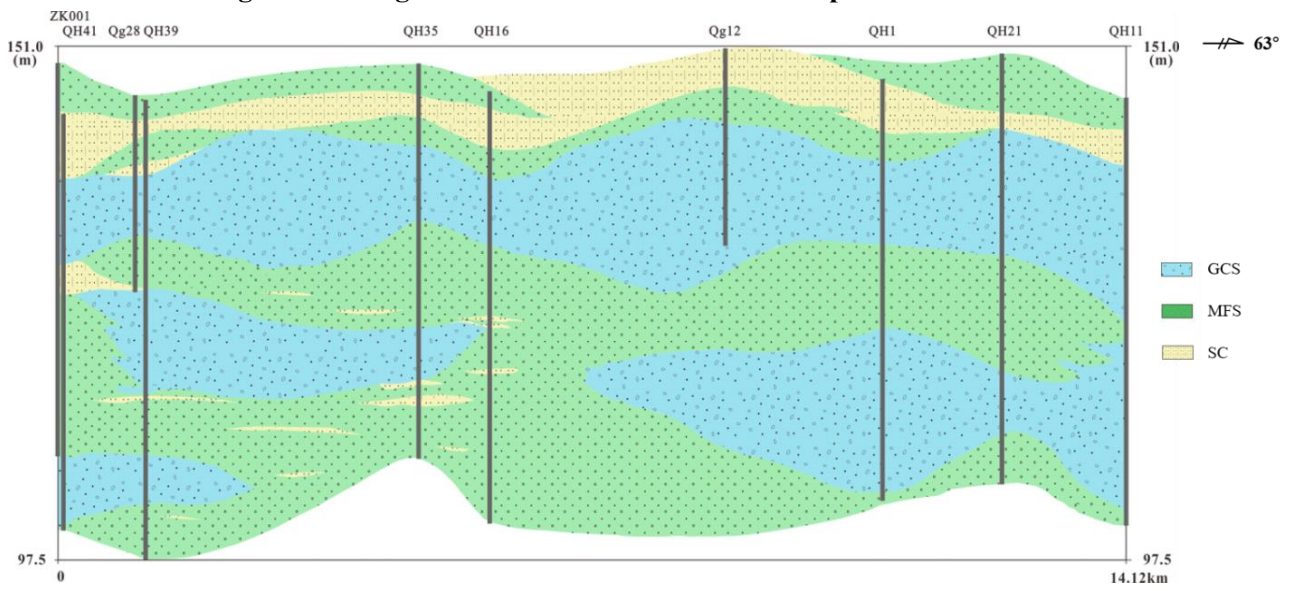


Figure S10. Large-scale lithofacies distribution map on cross-section 2.

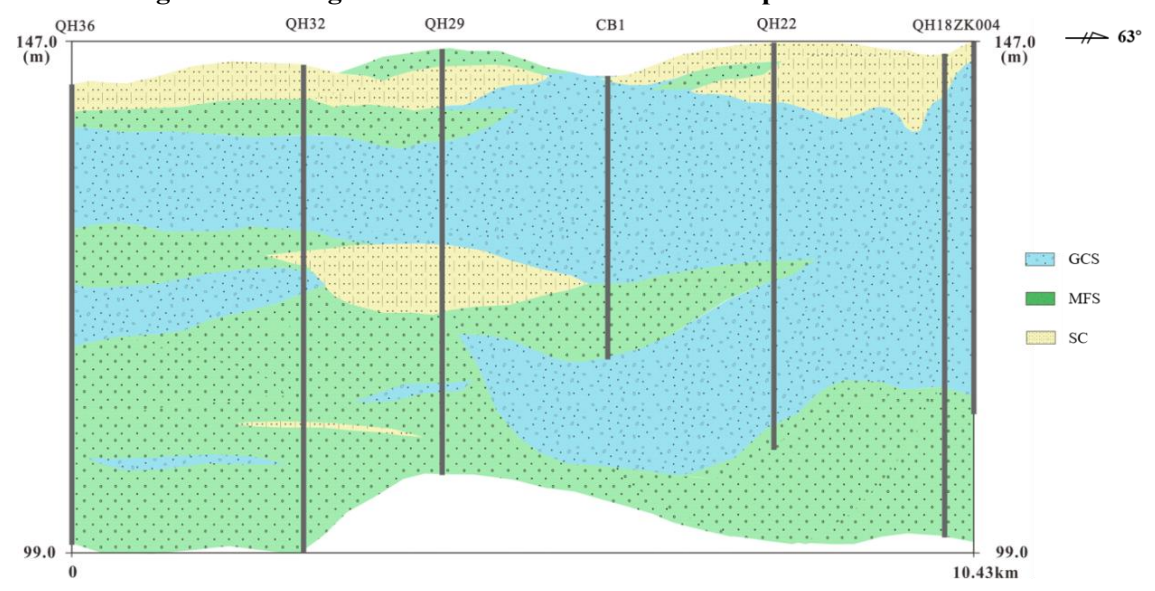


Figure S11. Large-scale lithofacies distribution map on cross-section 3.

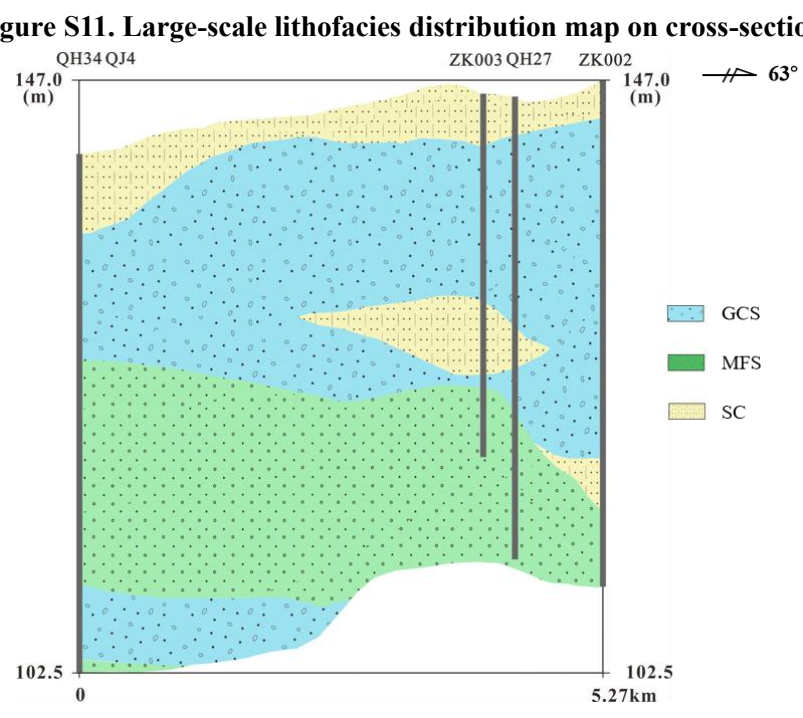


Figure S12. Large-scale lithofacies distribution map on cross-section 4.

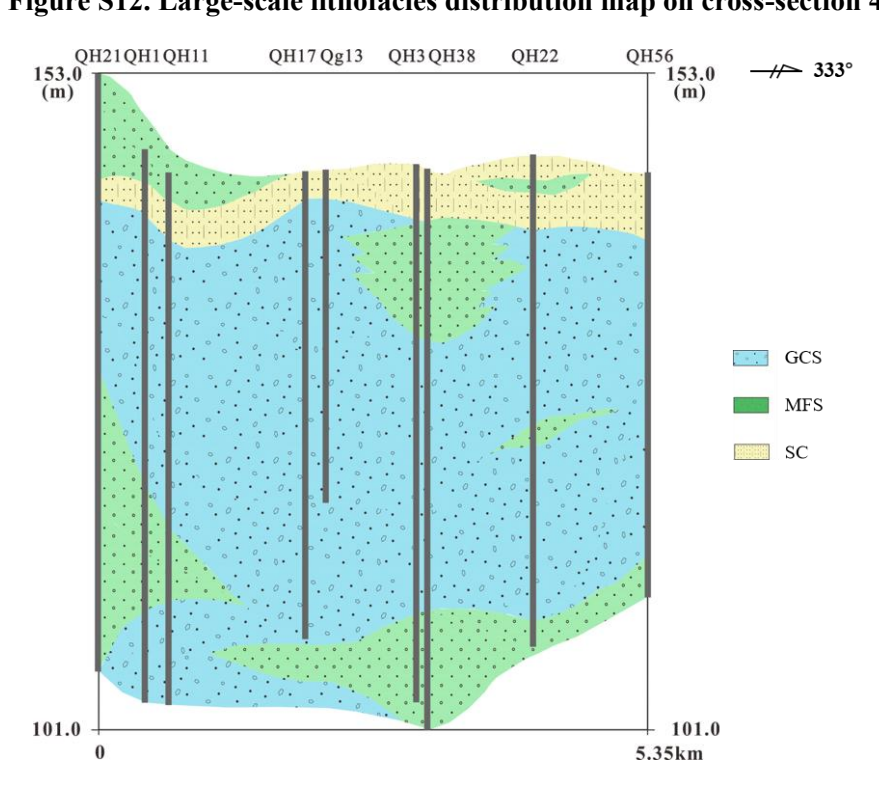


Figure S13. Large-scale lithofacies distribution map on cross-section 5.

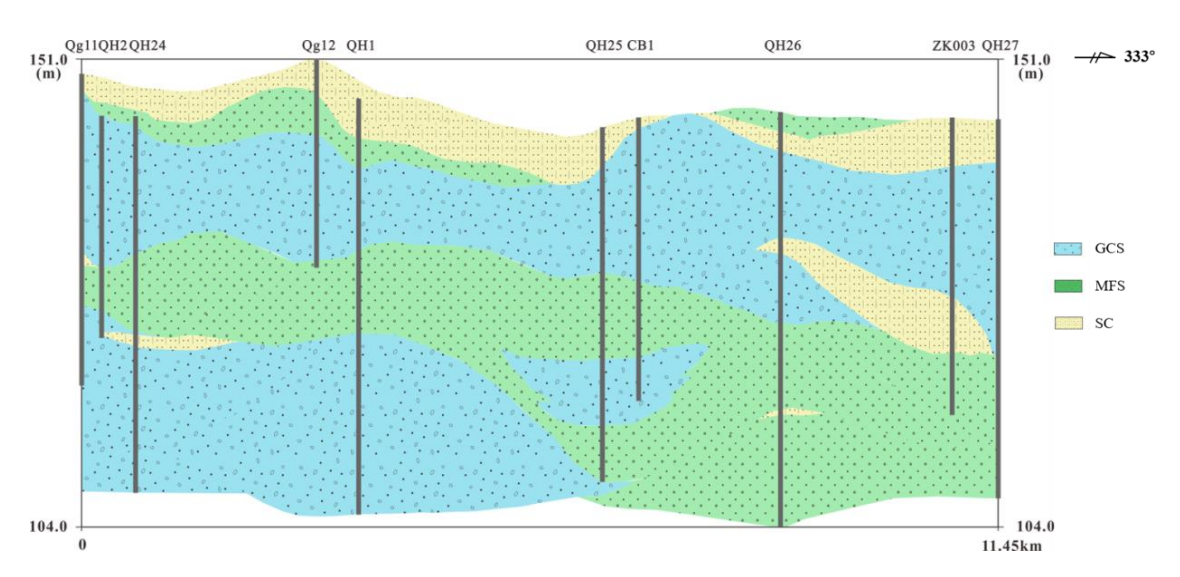


Figure S14. Large-scale lithofacies distribution map on cross-section 6. $_{QH35}$ $_{QH3}$ $_{QH31}$ $_{QH31}$ $_{QH32}$ $_{QH32}$ $_{QH33}$ $_{QJ4}$ $_{CK20}$ $_{CK20}$

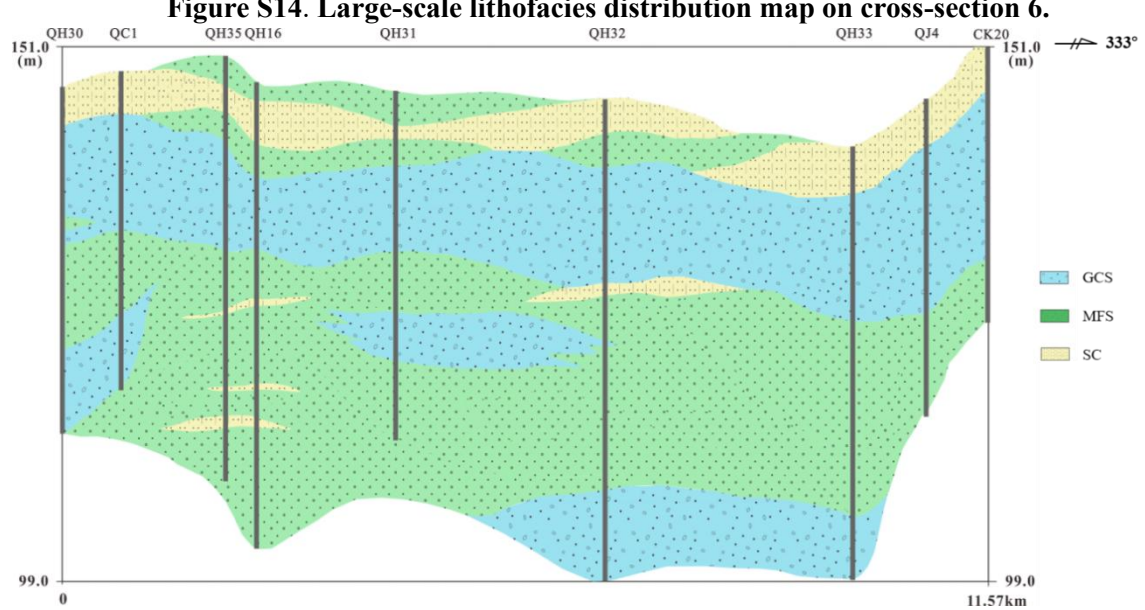


Figure S15. Large-scale lithofacies distribution map on cross-section 7.

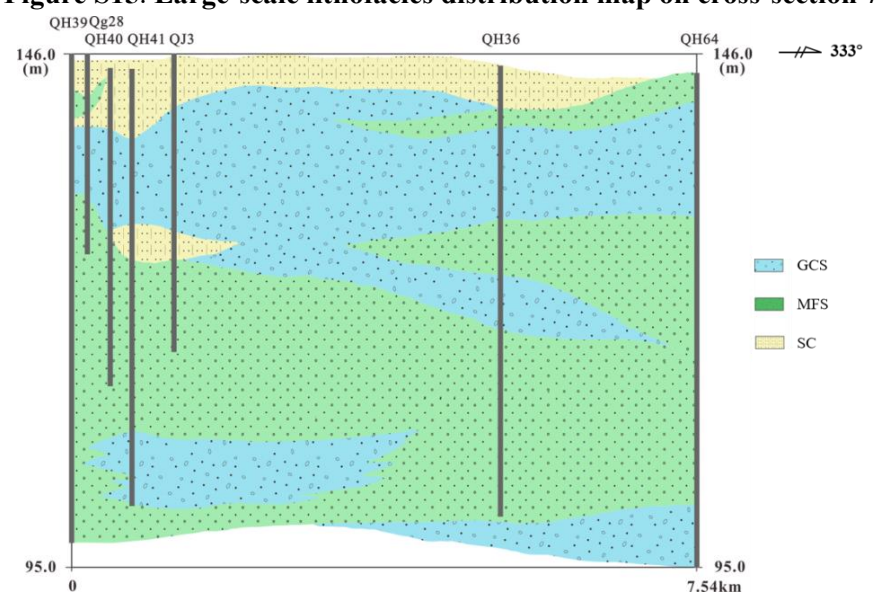


Figure S16. Large-scale lithofacies distribution map on cross-section 8.

Table S1. Proportionate values and errors of lithofacies volume counted in the boreholes and on the profiles of Scale I and Scale II

Scale	Facies type	P_D		P_S		P_D - Ps	
		X	Y	X	Y	X	Y
Scale I	G	0.349	0.332	0.358	0.328	-0.009	0.004
	CS	0.058	0.046	0.064	0.048	-0.006	-0.002
	MCS	0.082	0.137	0.081	0.138	0.001	-0.001
	MS	0.139	0.111	0.155	0.098	-0.016	0.013
	MFS	0.181	0.172	0.165	0.174	0.016	-0.002
	FS	0.088	0.076	0.079	0.093	0.009	-0.017
	SL	0.031	0.067	0.024	0.078	0.007	-0.011
	С	0.072	0.059	0.074	0.043	-0.002	0.016
Scale II	GCS	0.489	0.515	0.503	0.514	-0.014	0.001
	MFS	0.409	0.359	0.399	0.365	0.010	-0.006
	SC	0.103	0.126	0.098	0.121	0.005	0.005

Note: P_D is the volume proportion of lithofacies based on borehole statistics; P_S is the volume proportion of lithofacies based on profile statistics; P_D - P_S is the error value of the volume proportion of lithofacies based on borehole and profile statistics. When calculating using borehole data, the cumulative length of a phase is divided by the total statistical length of all lithofacies to obtain the volume proportion of that phase.

Table S2. Empirical methods for estimating the hydraulic conductivity from grain size

Fomula	$\varphi(n)$	d_e	C	Applicability	
Hazen	1+10(<i>n</i> -0.26)	d_{10}	6×10 ⁻⁴	0.10mm< <i>de</i> <3.00mm	
Slichter	$n^{3.287}$	d_{10}	0.01	0.01mm< de <5.00mm	
Pavichich	$\frac{n^3}{1-n^2}$	d_{17}	1	0.06mm< de <1.50mm	
Beyer	1	d_{I0}	$6\times10^{-4}\log(\frac{500}{\eta})$	0.06mm< de <0.60mm; 1<η<20	
Sauerbrei	$\frac{n^3}{1-n^2}$	d_{17}	3.75×10 ⁻³	Sands and sandy clay, $de < 0.50 \text{mm}$	
Kozeny	$\frac{n^3}{1-n^2}$	d_{10}	8.3×10 ⁻⁴	Large-grain sand	
USBR	1	d_{20}	$4.8 \times 10^{-4} (d_{20})^{2.3}$	Medium-grain sands	

[S1]. Source and sink calculation

Based on the recharge conditions of phreatic water, the lithology and thickness of the air-packed zone, building cover and cultivated land, a total of four water resources calculation zones have been delineated (shown in Figure 1b).

S1.1 Groundwater recharge term

S1.1.1 Lateral groundwater recharge (Q_{lg})

Lateral groundwater recharge from the east boundary is calculated by applying Darcy's formula:

$$Q_{lg} = KIML$$
 (S1)

Where: Q_{lg} is the amount of lateral groundwater recharge (10⁴m³/a); K is the equivalent conductivity of the aquifer (m/d); I is the hydraulic gradient of the groundwater; M is the average thickness of the aquifer (m); and L is the width of the lateral recharge section (m).

The conductivity is 61.46 m/d and the width of the inflow section is 20.57 km, the thickness of the aquifer on the boundary was taken as the average value of 32 m, and the hydraulic gradient is about 0.0009. The lateral recharge is then calculated to be $1328.96 \times 10^4 \text{m}^3/\text{a}$.

S1.1.2 Precipitation infiltration recharge (Q_P)

Calculations were made according to the 4 plots that were divided:

$$Q_{P} = \sum_{i=1}^{4} \alpha_{i} F_{i} P \tag{S2}$$

Where: Q_P is the amount of precipitation infiltration recharge (10^4 m³/a); α_i is the precipitation infiltration coefficient of subarea i (dimensionless), F_i is the area of subarea i (m²); and P is the multi-year average rainfall (m). The values of above parameters for each subarea are shown in Table A1. According to the rainfall monitoring data of Qiqihar City from 1990 to 2013, it is known that the multi-year average rainfall in the area is 437.7 mm.

Table 55 Calculation of Technique from precipitation									
Area	F (km ²)	α	$C_i(mm)$	$Q_P \ (10^4 \text{m}^3/\text{a})$					
1	66.7	0.28	437.7	817.3					
2	57.66	0.05	437.7	126.2					
3	117.17	0.2	437.7	1025.7					
4	189.09	0.15	437.7	1241.4					
Total	430.62			3210.6					

Table S3 Calculation of recharge from precipitation

S1.1.3 Mining return recharge (Q_M)

According to statistics, the total annual mining volume of phreatic water in the area is $2163.41 \times 10^4 \text{m}^3/\text{a}$, of which the agricultural water consumption is $915 \times 110^4 \text{m}^3/\text{a}$. The mining return coefficient is taken to be 0.3, so that the calculated mining return recharge volume is $274.50 \times 10^4 \text{m}^3/\text{a}$.

S1.2 Groundwater discharge term

S1.2.1 Evaporative emissions (Q_{ep})

Phreatic water evaporation is calculated using the evaporation coefficient method:

$$Q_{ep} = F\varepsilon, \varepsilon = \varepsilon_0 (1 - h/l)^n$$
 (S3)

Where: Q_{ep} is the amount of phreatic water evaporation discharge (10⁴m³/a); F is the area of evaporation zone (m²); ε is the phreatic water evaporation intensity (m/a); ε_0 is the water surface evaporation intensity (m/a); h is the phreatic water average depth of burial (m); l is the evaporation limit depth (m); n is the evaporation index related to the soil texture and climate of the air-bearing zone, and the value taken here is 1.

Only the evaporation during the thawing period is calculated. The limit depth of phreatic water evaporation in the area is 3m. Since the average depth of groundwater in subarea II is greater than 3m, so only subareas I, II, and IV are involved for calculation. The multi-year average evaporation ε_{θ} from April to September is 95lmm, and the multi-year average evaporation intensity $\varepsilon_{i} = \varepsilon_{\theta} \cdot F_{i} / F$ assigned to each sub-area. The results are shown in Table A2.

Area $F(km^2)$ $Q_{zp} (10^4 \text{m}^3/\text{a})$ $\varepsilon_i(m)$ h (m) l(m)66.7 0.15 1.79 3 397.8 3 117.17 0.26 202.1 2.8 3 4 189.09 0.42 2.79 3 552.7 Add up the total 372.96 1152.7

Table S4 Calculated results of evaporation discharge

Note. F is the area of the evaporation zone; ε_i is the water surface evaporation intensity; h is the average depth of groundwater; l is the maximum depth for groundwater evaporation.

S1.2.2 Vertical discharge (Q_V)

As the water level of confined groundwater in this study area is always lower than the water level of phreatic water, and accompanied by a large number of concentrated mining of confined groundwater, it increases the water level difference between phreatic water and confined groundwater so that the phreatic water under the action of the head pressure of the cross-flow recharge to the confined groundwater. The amount of discharge of the phreatic water is equal to the amount of recharge of the confined groundwater:

$$Q_V = FT\Delta H K'/M' \tag{S4}$$

Where: Q_V for phreatic water discharge (10⁴m³/d); F for the discharge area (m²); T is the time for leakage (d/a); ΔH for phreatic water and confined groundwater between the water level difference (m); K'/M' for the leakage coefficient (1/d).

Tthe average leakage coefficient is set as 0.0019(1/d) and the average water level difference ΔH between phreatic water and confined water is 0.7m. The area of the main interact zone is 68.6km^2 . The vertical discharge of phreatic water is calculated to be $3330.19 \times 10^4 \text{m}^3/\text{a}$.

S1.2.3 Groundwater extraction (Q_{ex})

The phreatic water is mainly used for irrigation, followed by production and domestic use. According to the report on groundwater dynamics in Qiqihar City (1990-2013), the average extraction amount of phreatic water is 2163.41×10⁴m³/a.